WAVELET ANALYSIS OF UNSTEADY CHARACTERISTICS IN SWIRLING GAS-PARTICLE FLOW

Hui Li
Department of Mechanical Engineering, Kagoshima University
1-21-40, Korimoto, Kagoshima City 890-0065, JAPAN
e-mail: li@mech.kagoshima-u.ac.jp

ABSTRACT

The multiresolution analysis and multiresolution cross-correlation analysis were applied to experimental pressure-time signals in this paper, in order to analyze the characteristics of swirling gas-particle two-phase flows in both Fourier and physical spaces. From randomlike pressure fluctuations, the fluctuating pressure components due to dune flow can be extracted over a time-scale plane based on the multiresolution analysis. It was found that the dominant scale of the heterogeneous suspension flow over the dunes increases along flow direction and reaches $0.017s$ in the fully developed region. The multiresolution cross-correlation analysis revealed that dunes with same moving velocity of $1 m/s$ pass through test pipeline and non-correlation existed at smaller scales that represent heterogeneous suspension flow over the dunes.

INTRODUCTION

Gas-particle two-phase flow systems are of considerable engineering importance, and have wide range industrial applications. Typical examples are the pneumatic conveying of materials and the coal energy conversion systems. Conventional pneumatic conveying, that is axial flow pneumatic conveying (AFPC) or axial gas-particle flow, is frequently operated in the dilute-phase regime in the high air velocity region. Power consumption, pipe erosion, and particle degradation considerations dictate that the conveying velocity be held to a minimum. In the last thirty-five years, there has been increasing interest in dense-phase pneumatic conveying, and several commercial systems have been developed. Unfortunately, these systems require high pressure drops and have high initial costs. Furthermore, dense-phase pneumatic conveying may lead to unstable flows at low conveying velocities. These unstable flows often cause blockage and pipe vibration.

To reduce power consumption, blockage, particle degradation and pipe wear, this new swirling flow technique, called swirling flow pneumatic conveying (SFPC) or swirling gas-particle flow, was applied to horizontal and vertical pneumatic conveying by Li and Tomita (1996, 1998). In the low velocity conveying range, SFPC was determined to be effective.

However, swirling gas-solid two-phase flows are unsteady and complicated nonlinear dynamics system. A detailed understanding of the behavior of particles is importance for design, optimization and operation of swirling flow pneumatic conveying system. The prediction or identification of particle flow patterns is one of the important problems. Usually, the flow pattern maps of gas-particle flows are based on the visual identification of phase distribution. Although identification of visual flow patterns may be adequate for some cases (Li and Tomita 1996, 1998), in many situations these methods are not applicable or are too subjective. Several other methods have been developed to more objectively identify and interpret flow patterns and transitions of two-phase flow (Li and Tomita 1997), e.g., pressure-time signals, root mean square (RMS) of pressure-time series, auto and cross correlation function, skewness and flatness factor, the power spectral density function (PSD), and probability density function (PDF). These studies have contributed to our understanding of flow patterns and transitions of two-phase flow in statistics, but they are utterly incapable of dealing properly with particle flow patterns that is change over time. Although particle flow patterns may be identified by the observation, the unsteady characteristics of gas-particle flows that the local scale with respect to space-time changes continuously cannot be qualitatively determined yet.

It is well known that pressure signals contain sufficient information on peculiar features of flow pattern and unsteady characteristics of gas-particle flows. Until now, the traditional techniques lost the information on the time for obtaining statistical characters, and are inadequate for unsteady flow.

The aim of this paper is first to apply the multiresolution analysis approach to the experimental data of pressure-time signals in a horizontal swirling gas-solid flow and to study the characteristics of the wall pressure fluctuation in both Fourier and physical spaces. Then the multiresolution cross-correlation analysis is developed and is employed to extract the most essential scales governing the correlation features.

DISCRETE WAVELET TRANSFORM

In this session, a brief review of the discrete wavelet transform is introduced from the view of matrix.

The discrete wavelet transform is a transformation of information from a fine scale to a coarser scale by extracting information that describes the fine scale variability (the detail coefficients or wavelet coefficients) and the coarser scale smoothness (the smooth coefficients or mother-function coefficients) according to:

$$\{S_j\}=[H]\{S_{j+1}\} \quad ; \quad \{D_j\}=[G]\{S_{j+1}\} \tag{1}$$

where S represents mother-function coefficients, D represents wavelet coefficients, j is the wavelet level, and H and G are the convolution matrices based on the wavelet basis function. High values of j signify finer scales of information. The complete wavelet transform is a process that recursively applied Equation (1) from the finest to the coarsest wavelet level (scale). This describes a scale by scale extraction of the variability information at each scale. The mother-function coefficients generated at each scale are used for the extraction in the next coarser scale.

The inverse discrete wavelet transform is similarly implemented via a recursive recombination of the smooth and detail information from the coarsest to finest wavelet level (scale):

$$\{S_{j+1}\}=[H]^T\{S_j\}+[G]^T\{D_j\} \tag{2}$$

where H^T and G^T indicate the transpose of H and G matrices, respectively.

The matrices H and G are created from the coefficients of the basis functions, and represent the convolution of the basis function with the data.

Many different orthonormal wavelet basis functions, such as the Harr basis, Daubechies basis, Meyer basis, Spline basis, and Coiflets basis, were often used in the discrete wavelet transform. Different wavelet basis functions will preferentially move, between scales, different characteristics of the target data sets. Such as, use of The Harr basis function may emphasize discontinuous in the target data sets, and the Daubechies family may emphasize the smoothness of the analyzed data. In this paper, we use the Daubechies family as the wavelet basis function. The simplest (and most localized) member called Daubechies wavelet with orders 4, which has only four coefficients, c_0, c_1, c_2 and c_3, is given, by the following matrix.

$$\begin{bmatrix}
c_0 & c_1 & c_2 & c_3 & & & & & & & \\
c_3 & -c_2 & c_1 & -c_0 & & & & & & & \\
 & & c_0 & c_1 & c_2 & c_3 & & & & & \\
 & & c_3 & -c_2 & c_1 & -c_0 & & & & & \\
\cdot & \cdot & & & \cdot & & & & & & \\
\cdot & \cdot & & & & \cdot & & & & & \\
\cdot & \cdot & & & & & \cdot & & & & \\
 & & & & & & & c_0 & c_1 & c_2 & c_3 \\
 & & & & & & & c_3 & -c_2 & c_1 & -c_0 \\
c_2 & c_3 & & & & & & & & c_0 & c_1 \\
c_1 & -c_0 & & & & & & & & c_3 & -c_2
\end{bmatrix} \tag{3}$$

where blank entries signify zeroes. The action of the matrix, overall, is thus to perform two related convolutions, then to decimate each of them by half and interleave the remaining halves. It is useful to think of the coefficient c_0, c_1, c_2 and c_3 as being a smoothing filter called it matrix H, something like a moving average of four points. Then because of the minus signs, coefficient c_3, $-c_2$, c_1 and $-c_0$, call it matrix G, is not a smoothing filter.

In this study, Daubechies wavelet with orders 20 is used as orthonormal wavelets, since a high order wavelet base have good frequency localization that in turn increases the energy compaction.

MULTIRESOLUTION ANALYSIS

Since Mallat first applies multiresolution analysis to the field of image processing, researchers have been making widespread use of multiresolution analysis for several years. The goal of the multiresolution analysis is to get a representation of a signal that is written in a parsimonious manner as a sum of its essential components.

It is well known that a signal often includes too much information for real time vision processing. Multiresolution algorithm process fewer data by selecting the relevant details that are necessary to perform a particular recognition task. That is, a parsimonious representation of a signal will preserve the interesting features of the original signal, but will express the function in terms of a relatively small set of coefficients. Thus overcoming limitations of the continuous wavelet transform that cannot reconstruct the original signal. Coarse to fine searches processes first a low-resolution signal and zoom selectively into finer scales information.

In mathematics, the multiresolution analysis consists of a nested set of linear function spaces V_j with the resolution of functions in increasing with j. More precisely, the closed subspaces V_j satisfy

$$\cdots V_2 \subset V_1 \subset V_0 \subset V_{-1} \subset V_{-2} \cdots \tag{4}$$

$$\text{with} \quad \overline{\bigcup_{j\in Z} V_j} = L^2(\Re^2) \quad \text{and} \quad \bigcap_{j\in Z} V_j = \{o\} \tag{5}$$

The basis functions for the subspaces V_j are called scaling functions of the multiresolution analysis.

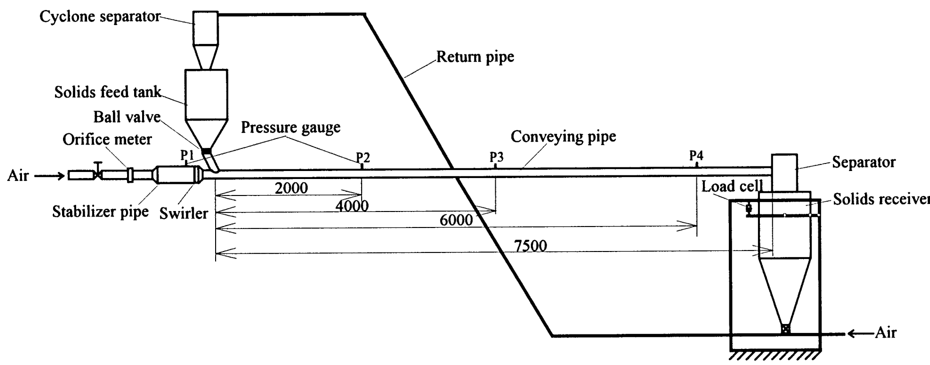

Figure 1. Experimental equipment.

For every $j \in Z$, define the wavelet spaces W_j to be the orthogonal complement of in V_{j-1} of V_j. We have

$$V_{j-1} = V_j \oplus W_j \tag{6}$$

and

$$W_j \perp W_{j'} \quad \text{if} \quad j \neq j'. \tag{7}$$

i.e., any function in V_{j-1} can be written as the sum of a unique function in V_j and a unique function in W_j. In $L^2(\Re^2)$, the orthogonal basis for W_j is the family of wavelets that is defined. Thus, $L^2(\Re^2)$ can be decomposed into mutually orthogonal subspaces, and can be written as

$$L^2(\Re^2) = \bigoplus_{j \in Z} W_j \tag{8}$$

In this study, the procedure of this multiresolution analysis can be summarized in two steps:

(1) Wavelet coefficients of a signal are computed based on the discrete wavelet transform of Eq.(1).
(2) Inverse wavelet transform of Eq.(2) is applied to wavelet coefficients at each wavelet level, and components of signal are obtained at each level or scale.

Of course, a sum of these essential components of signal can recover the original signal.

EXPERIMENTAL APPARATUS AND PROCEDURE

In this study the experimental facility is the pressurized system and is shown schematically in Fig.1. Air from a blower flows through the calibrated nozzle and a vaned swirler in the stabilizer pipe, and picks up the solid materials fed by gravity from the feed tank at the inlet of conveying pipeline. Then, the solids-air mixture enters the conveying pipeline and at the pipeline exit the solids are separated from the solids-air mixture by the separator. The conveying pipeline consisted of a horizontal smooth acrylic tube of 76*mm* inside diameter and about 7500*mm* length.

The airflow rate was measured by the orifice meter, and the fluctuation of solid mass flow rate was measured by a load cell. The fluctuations of static pressure along the pipeline were measured at locations *L*=2*m*, 4*m* and 6*m* from the solid feed point by use of semiconductor pressure transducers, whose frequency response is 800*Hz*. The data length of 8000 points for each test case was utilized to carry the wavelet analysis. Polyethylene pellets of 3.5*mm* and a density of 1210kg/m^3 were used as test solids. The mean air velocity U_a was from 6*m/s* to 28*m/s* and the solid mass flow rate G_s from 0.3*kg/s* to 0.5*kg/s*. The initial swirl number S_0, which was defined at the inlet of conveying pipeline and calculated using author's method (Li and Tomita 1994), was varied from 0.00-0.61.

RESULTS AND DISCUSSION

Total Pressure Drop

The same as the previous papers (Li and Tomita 1996), the total pressure drop Δp_t contains the pressure drop due to the vaned swirler, i.e., the total pressure drop between the stabilizer pipe and the exit of conveying pipe is considered. For steady state flow, Δp_t can be obtained as follows:

$$\Delta p_t = \Delta p_1 - \frac{1}{2}\rho_a\left[1-\left(\frac{D}{D_0}\right)^4\right]U_a^2 \tag{9}$$

where Δp_1 is the wall static pressure of stabilizer pipe before the vaned swirler, D and D_0 are the diameters of pipeline and stabilizer pipe, respectively.

Figure 2 shows the total pressure drop versus the air velocity with the initial swirl number S_0 as a parameter for the solids mass flow rate 0.5*kg/s*. According to S_0, three kinds of SFPC are called swirl 1 flow (S_0=0.28), swirl 2 flow (S_0=0.49) and swirl 3 flow (S_0=0.61), respectively. From Fig.2 it is evident that the minimum and critical velocity of SFPC are smaller than that of AFPC. The same as AFPC the pressure drop of SFPC firstly decreases and then rises below the minimum velocity, when air velocity decreases. Comparing SFPC with AFPC in Fig.2, the pressure drop of SFPC is higher than that of AFPC in range of high air velocity. However, below and near the minimum velocity of SFPC, the pressure drops of swirl 1 and swirl 2 flow become

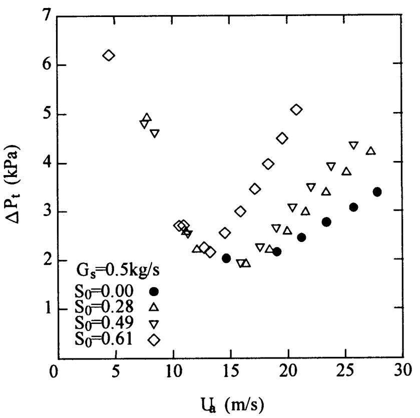

Figure 2. Relation between the total pressure drop and air velocity.

lower than that of AFPC. On the other hand, swirl 1, swirl 2 and swirl 3 flow show same pressure drop in range of low air velocity due to the weak swirl flow.

Classification of Flow Patterns

In the present work we attempt to reveal the unsteady features of the horizontal swirling gas-solid flow from the picture of flow patterns transitions with time-frequency localization. Corresponding to the variation of the air velocity, as described in Li and Tomita (Li and Tomita 1996), six main flow patterns of particles in this experiment are defined:

①*Fully swirling suspended flow* - at high air velocities.
②*Strand sliding flow* – at medium air velocity.
③*Clusters sliding flow* - after a certain air velocity.
④*Dune flow* – at low air velocity.
⑤*Flow with a stationary bed* - at even lower air velocity.
⑥*Plug flow* - further reduction of air velocity.

Although there are other factors (e.g. the mass load ratio, swirl number and particle properties) that govern the various flow patterns, the flow patterns are discussed to depend simple on the air velocity in this study.

Multiresolution Analysis of Pressure Fluctuations

It is well known that the unsteady characteristics of the swirling gas-particle flow are especially important in the low air velocity range. In this paper we first discussed transitions of dune flow pattern ④ in the acceleration and fully developed regions.

The components of wall pressure fluctuations for U_a=8.66*m/s*, G_s=0.3*kg/s* and S_0=0.61 at locations x=2*m* from the particle feed point along flow direction ranged from wavelet level 1 to 8, which correspond to scale range a=0.01~2.5*s*, are shown in Fig.3 (a). The time history data of wall pressure was also plotted in this figure. This figure represents the time behavior of the fluctuating wall pressure within different scale bands. The obvious nearly periodic

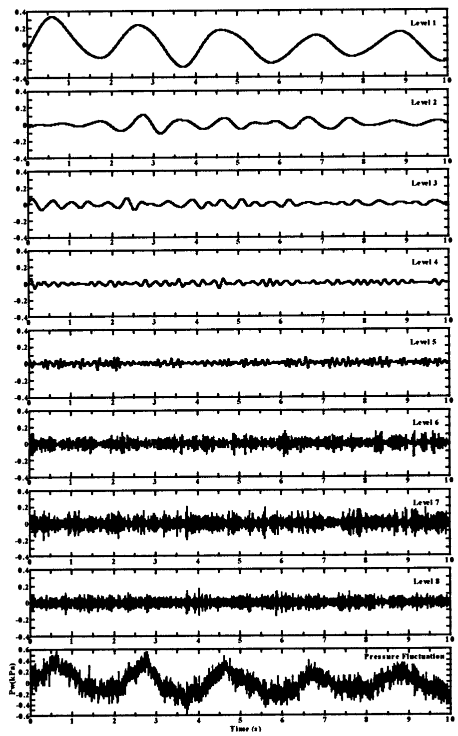

Figure 3(a). Multiresolution decomposition of fluctuating pressure at locations x=2*m*.

large peaks are observed at wavelet level 1, which corresponds to scale a=1.7~2.5*s* and centers at a=2.5*s* approximately. These peaks imply the occurrence of the dune flow patterns of ④ in the acceleration region, and the scale range is dynamically quite important and dominates the character of flow. The positive peaks represent the passing dune at this moment, and the negative peaks indicate the interval between two successive dunes. The larger amplitude of positive peaks implies a larger dune. The fluctuating pressure components due to dune flow can be extracted from original pressure signal based on the multiresolution analysis. Making a comparison between components of wall pressure fluctuations and original wall pressure fluctuation, we find that alternative large positive and negative peaks at level 1 correspond to the positive and negative peaks of the large scale in the original wall pressure fluctuation, respectively. Comparing with other fluctuating pressure components, the larger alternative peaks of the fluctuating pressure component are also observed at level 7, which corresponds to scale a=0.02~0.06*s* and centers at a=0.03*s* approximately. These peaks indicate the heterogeneous suspension flow that occupies the rest of pipe over the dunes.

At a downstream distance of x=4*m*, as shown in Fig.3 (b), the periodic peaks at level 1 that result from the occurrence of the dune flow patterns of ④ are also appeared. The amplitude of positive peaks are almost same, and the flow characteristics may be interpreted the existence of the dunes along the bottom of the pipe at nearly const intervals. Another dominate scale, which results from heterogeneous

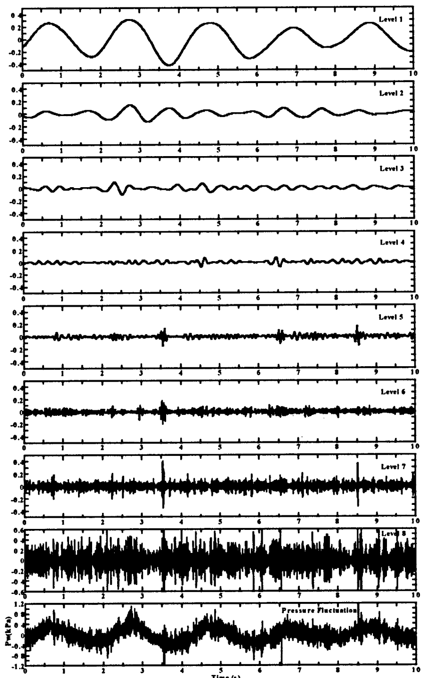

Figure 3(b). Multiresolution decomposition of fluctuating pressure at locations x=4m.

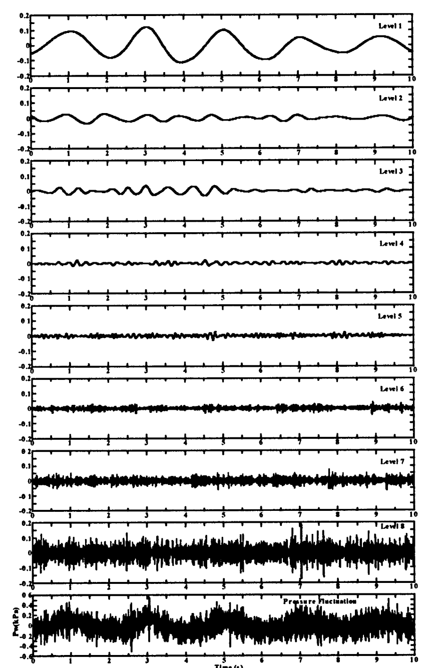

Figure 3(c). Multiresolution decomposition of fluctuating pressure at locations x=6m.

suspension flow over the dunes, increase and appear at level 8 that corresponds to scale a=0.009~0.025s and centers at a=0.017s approximately, because the particle velocities are accelerated.

In the fully developed region at x=6m, as shown in Fig.3(c), the dominate scales of the dunes and the heterogeneous suspension flow exist at level 1 and 8, respectively, however, the amplitude of peaks decreases. This exhibits that the periodic dune become smaller and the fluctuation of particle velocities in the heterogeneous suspension flow become weaker in the fully developed region.

From above analysis, we find that the flow characteristics focus on the wavelet level 1 (large scale) and level7 or 8 (small scale) in the lower air velocity range.

Multiresolution Cross-Correlation Analysis of Pressure Fluctuations

In identifying the spatial structure of signals and its evolution in time, the cross-correlation analysis between two signals is most used. A difficulty with the conventional cross-correlation method, however, is that the cross-correlation function only provides information about the cross-correlation behavior in terms of time delay but no information about correlation behaviors in scale space due to lack of scale resolution. Recently, Li (1998) developed wavelet cross-correlation analysis based on the continuous wavelet transform. The wavelet cross-correlation analysis provides the unique capability for decomposing the correlation of arbitrary signals over a two-dimensional time delay-period plane. In analogy with the wavelet cross-correlation, in this study we first unfold respectively two different signals into their two-dimensional time-scale planes using multiresolution analysis. Then we use two signal components coming from different signals with same wavelet level to define a cross-correlation function, called the *multiresolution cross-correlation function.*

Figure 4(a) shows the multiresolution cross-correlation coefficients of wall fluctuating pressures between the location x=2m and 4m for U_a=8.66m/s, G_s=0.3kg/s and S_0=0.61. The conventional cross-correlation coefficients are also included. It is evident that the distribution of conventional cross-correlation coefficients is similar to multiresolution cross-correlation coefficients of level 1, however, its amplitude is smaller than that of multiresolution cross-correlation coefficients and cannot provide cross-correlation information at other scale. The multiresolution cross-correlation coefficients describe this fact that the cross-correlation becomes weaker as the wavelet level increases or scale decreases. The stronger correlation exists at level 1 and 2, and implies periodic motion of dune within these two scale ranges. The moving velocities of dunes may be calculated based on multiresolution cross-correlation, and give 1m/s and 2m/s, respectively.

The multiresolution cross-correlation coefficients of wall fluctuating pressures between the location x=4m and 6m is shown in Fig.4 (b). The conventional cross-correlation coefficients become smaller than that of Fig.4 (a). The multiresolution cross-correlation coefficients of level 1 remain the larger correlation, and the moving velocities of dunes computed from distribution of peaks are same as Fig.4

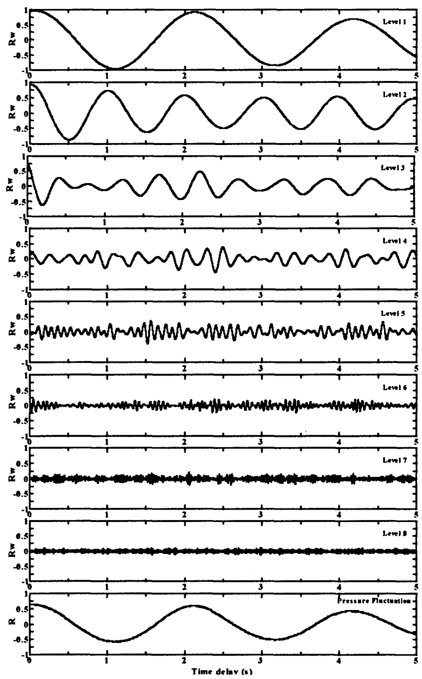

Figure 4 (a). Multiresolution cross-correlation of fluctuating pressures between the location x=2m and 4m.

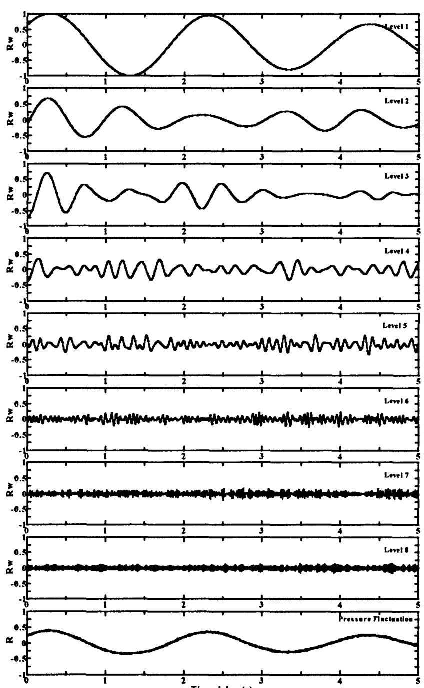

Figure 4 (b). Multiresolution cross-correlation of fluctuating pressures between the location x=4m and 6m.

(a). This indicates that the dunes with same moving velocity pass through the test pipeline. The multiresolution cross-correlation of level 2 becomes weaker. Although stronger peaks are observed in the fluctuating pressure components of level 8 in Figs.3 (b) and (c), which represent heterogeneous suspension flow over the dunes, the non-correlation is found at level 8. This may be interpreted as the random motion of particles.

It is clear that the multiresolution cross-correlation analysis can provide the information on correlation at various scales, and extract the most essential scales governing the correlation features, which is difficulty if using conventional method.

CONCLUSIONS

The multiresolution analysis and multiresolution cross-correlation analysis were applied to experimental pressure-time signals, in order to analyze the characteristics of swirling gas-particle two-phase flows in both Fourier and physical spaces. The main conclusions can be summarized as follows:

(1) From randomlike pressure fluctuations, the fluctuating pressure components due to dune flows can be extracted based on the multiresolution analysis over a time-scale plane.

(2) The dominant scale of the heterogeneous suspension flow over the dunes increases along flow direction and reaches 0.017s in the fully developed region.

(3) The multiresolution cross-correlation analysis can provide the information on correlation between two different signals at various scales, and reveals that dunes with same moving velocity of 1m/s pass through test pipeline.

(4) Non-correlation was found at smaller scales that represent heterogeneous suspension flow over the dunes.

ACKNOWLEGMENT

This work was supported by The Asahi Glass Foundation.

REFERENCES

Li, H., 1998, "Identification of Coherent Structure in Turbulent Shear Flow with Wavelet Correlation Analysis", ASME *Journal of Fluids Engineering*, Vol.120, No.4, pp.778-785.

Li, H. and Y., Tomita, 1994, "Characteristics of Swirling Flow in a Circular Pipe", ASME *Journal of Fluid Engineering*, Vol. 116, No.2, pp. 370-373.

Li, H. and Tomita, Y., 1996, "An Experimental Study of Swirling Flow Pneumatic Conveying System in a Horizontal Pipeline", ASME *Journal of Fluid Engineering*, Vol.118, No.3, pp.526-530.

Li, H. and Tomita, Y., 1997, "Statistical Analysis of Pressure Fluctuation in Swirling Gas-Solid Two-Phase Flow in a Horizontal Pipe", *Modern Techniques and Measurements in Fluid Flows*, International Academic Publishers, pp.289-293.

Li, H. and Tomita, Y., 1998, "An Experimental Study of Swirling Flow Pneumatic Conveying System in a Vertical Pipeline", ASME *Journal of Fluids Engineering*, Vol.120, No.1, pp.200-203.